Discrete Medial Axis Transform for Discrete Objects

Anna Puig Puig

1 Introduction

The Medial Axis Transform MAT was defined by Blum in [Blu67] as an alternate description of the shape of an object. The MAT is the closure of the set of centers of maximal balls which can fit inside the object. A ball is maximal if it is not contained by any other such ball. This model is homotopic with the object characteristics and it is continuous if the object is path-connected ([SPW96]). It is a unique and a complete model representation. In addition, it provides dimensionality reduction, symmetry detection and invertibility. Thus, it is an alternate compressed representation of objects and it preserves their topological characteristics. This is the reason why this description has been shown to be useful in CAD designs in order to reduce the computational complexity of certain algorithms. Nevertheless, it is a not minimal scheme and it is sensitive to small changes on the boundary of the object. Moreover, progress on its use has been limited by the difficulty of developping a robust, accurate and efficient algorithm for its construction.

In many applications of 2D digital image processing, discrete approximations of the MAT, such as skeletal representations, are used as decompositions of discrete objects whose width is not negligible and may vary. The main construction algorithms of these skeletons are thinning ([LLS92], [CCS95], [KSKB95], [LKC94]) and morphological methods ([MMD96]). These skeletons are continuous but they do not reflect all the topological features of the discrete objects and they are not complete representation schemes.

Other skeletal schemes are based on Distance Map transformations (DM) extrapolating Blum's definition to the discrete case ([Dan80], [KSKB95]). These skeletons constitute complete representation models but they do not preserve the connectivity of the axis in order to find a minimal and compressed scheme representation ([ND97]). Even though the compression is a goal to attain, the preservation of the connectivity is essential to keep up the topological characteristics of the object boundary in order to apply algorithms such as those that realize pattern recognition directly on the skeleton instead of on the object boundary. Furthermore, as computing the distance from a pixel to a set of feature pixels is essentially a global operation, these algorithms are based on full scans of the images and, thus, their computational cost is proportional to the size of the image.

In this report, a Discrete Medial Axis definition is proposed as a direct extension of Blum's definition in order to achieve a complete and compressed model representation of discrete objects which retains the significant features of the object without introducing distorsions of its own. Moreover, it preserves the axis connectivity and it is based on local properties of the Distance Map which enable to design a seed algorithm for its construction whose cost is linear with the size of the object.

First, in section 2, some definitions and properties are reviewed. In section 3, the Discrete Medial Axis Transform for 2D discrete objects is defined and its main properties are demonstrated. The algorithm of the MATD construction is proposed in section 4 and its evaluation and some simulations are analyzed in sections 5 and 6 respectively. The 3D-extension of the definition and of the algorithm is discussed in section 7. Finally, the conclusions and the future work are presented in section 8.

2 Definitions and review

Before the definition of the Discrete Medial Axis Transform, it is necessary to state briefly some important definitions of basic concepts from digital topology and some hypothesis about the initial digital objects.

Let $\Re^2$ be the set of ordered pairs of floating numbers and let Z^2 be an integer subdivision of $\Re^2$, then a **pixel**, p_{ij} is a closed square in $\Re^2$. Each pixel is represented as a pair (i, j), which corresponds to the coordinates of the pixel central point in Z^2.

An **image**, I, is a structure (P, γ) where P is the domain of the scene (or set of pixels) and γ is the density function such that $\gamma(p_{ij})$ is the density value at the pixel $p_{ij} \in P$:

$$\gamma : p_{ij} \rightarrow [0, 1]$$

$$\begin{aligned} P = \quad \{p_{ij}/ \quad & X_l \leq i \leq X_h, X_l > 0, X_h > 0 \ \& \\ & Y_l \leq j \leq Y_h, Y_l > 0, Y_h > 0\} \end{aligned}$$

where X_l, Y_l, X_h i Y_h are the minimum and maximum values of the coordinates respectively.

The **borders of an image** are considered as:

$$\begin{aligned} border(I) = \quad \{p_{ij}/ \quad & i = X_l \ || \ i = X_h \ || \\ & j = Y_l \ || \ j = Y_h \ \} \end{aligned}$$

and it is assumed that $\forall p_{ij} \in border(I), \gamma(p_{ij}) = 0$.

Let O be a discrete object on an image I represented by a 8-connected set of pixels ([KR89]) such that its $\gamma(p_{ij}) = 1$, then the boundary of the object on the image is:

$$
\begin{aligned}
boundary(O) \;&=\; \{p_{ij}/p_{ij} \in O \; such \; that \;\; \gamma(p_{ij}) = 1 \\
&\;\;\; \& \;\;\; \exists p_{i'j'} : \gamma(p_{i'j'}) = 0 \; such \; that \\
&\;\;\;\;\;\;\;\; p_{i'j'} \in 8neighbour(p_{ij})\}
\end{aligned}
$$

Moreover, two object pixels are adjacents only if they are 8-adjacent and two non-object pixels are adjacent only if they are 4-adjacent. This statement avoids ambiguities in the classification of a pixel as interior or exterior to the digital object ([KR89]).

There are various discrete distance functions in the discrete space which approximate the continuous euclidian metric. Not all of these metrics define distances in mathematical sense, as they do not fullfil the triangular inequality. With any of these distance functions, the **distance from a pixel p_{ij} to a pixel set C** can be considered as:

$$dist(p_{ij}, C) = minimum_{p_{i'j'} \in C}\{dist(p_{ij}, p_{i'j'})\}$$

Def 1. The **distance map** of an image, I, referred to an object, O is the function:

$$DM : I \rightarrow \Re^{+}$$

which associates to every pixel of I the value of the minimum distance between the pixel and the boundary of the object O:

$$DM(p_{ij}) = \begin{cases} dist(p_{ij}, boundary(O)) & \text{if } p_{ij} \in O \\ 0 & \text{if } p_{ij} \in \bar{O} \end{cases}$$

Def 2. A discrete **disk** $D_t(p_{ij})$ of center (i, j) and radius t, is the set of the pixels which are at a distance from the pixel p_{ij} minor than a value t:

$$D_t(p_{ij}) = \{p_{i+h\,j+k}/dist(p_{ij}, p_{i+h\,j+k}) \leq t\}$$

According to the definition of the Medial Axis Transform given by [Blu67], a discrete skeleton can be defined on the basis of the distance notion as:

Def 3. Given O a 2D discrete object, **skeleton(O)** is defined as the set of pixels which are centers of maximum-sized disks fitted into O, i.e. disks that cannot be completely covered by any other larger disk fitted into O.

The most useful metrics cited in the bibliography ([Chi92], [Bor86], [Bor84]) are:

- n-neighbour distance: All local distances between neighbours are set to either 1 or to infinity. In two dimensions there are two versions, 4 and 8 neighbour distances:
  - 4-neighbour or maximum distance (city-block):

$$dist_{max}(p_{x_0,y_0}, p_{x_1,y_1}) = max\{fabs(x_1 - x_0), fabs(y_1 - y_0)\}$$

$$D_t(p_{ij}) = \{p_{i+h\,j+k}/max(h, k) \leq t\}$$

– 8-neighbour or absolute distance (chessboard):

$$dist_{abs}(p_{x_0,y_0}, p_{x_1,y_1}) = fabs(x_1 - x_0) - fabs(y_1 - y_0)$$

$$D_t(p_{ij}) = \{p_{i+h\,j+k}/fabs(h-k) \leq t\}$$

These distances are approximations of the Euclidean distance and in a $(M+1) \times (M+1)$ area of pixels, they differ from the Euclidean distance between $(\sqrt{2}-2) \times M$ and $-(\sqrt{2}-1) \times M$ respectively. The 4-neighbour distance is always greater than the Euclidean one, while the 8-neighbour distance is always smaller. A mixture of 4 and 8 neighbour distances is the octogonal distance. The disks become octagons. The upper limit of the error in an $(M+1) \times (M+1)$ area, for $M > 5$, is $(\sqrt{5}/2 - 1) \times M$.

- Chamfer distance: The local distances at a 4-neighbour and at a 8-neighbour are the real numbers d_1 and d_2. If $d_1 = 1$ and $d_2 = \sqrt{2}$, the upper limit of the difference with the Euclidean distance in an $(M+1) \times (M+1)$ area is $(\sqrt{2\sqrt{2}-2} - 1) \times M$. There are best approximations of the Euclidean distance such as $d_1 = 1$ and $d_2 < 2$ and there are good integer approximations which set d_1 to 2 and d_2 to 3.

- Euclidean distance [Dan80]:

$$dist_E(p_{x_0,y_0}, p_{x_1,y_1}) = (fabs(x_1 - x_0), fabs(y_1 - y_0))$$

$$D_t(p_{ij}) = \{p_{i+h\,j+k}/h^2 + k^2 \leq t^2\}$$

This metric gives the exact distance but two integer values must be stored for each pixel.

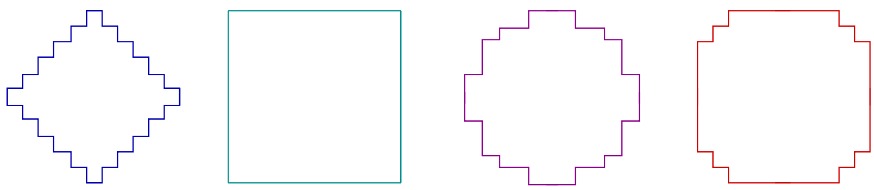

(a) (b) (c) (d)

Figure 1: Different neighbourhood shapes, radius 6 units: (a) City-block, (b) Chessboard, (c) Chamfer Distance and (d) Euclidean Distance.

The above defined metrics use different pixel neighbourhoods that approximate, more o less accurately, the shape of a continuous euclidean disk. Figure 1 shows the differents shapes of the disks according to the metric used.

Proposition 1. *The discrete skeleton computed with any discrete metric (n-neighbours, chamfer and euclidean distance) is not always connected.*

The examples shown in Figure 2 illustrate the above proposition.

The fact that the skeleton is not connected disables continuous traversals of the structure along it. In particular, its computation must be based on a global scan

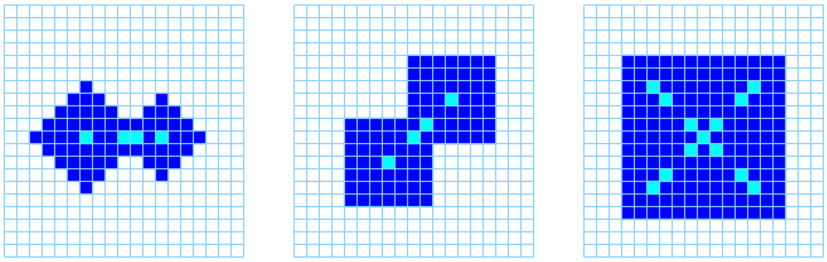

(a) city-block (b) chessboard (c) euclidian

Figure 2: Skeletons computed with different metrics.

of the image and it is not possible to perform a local strategy which would have a lower computational cost. It must be considered that these disconnections are not bounded by a neighbourhood instead, they may appear in cases such as of Figure 3.

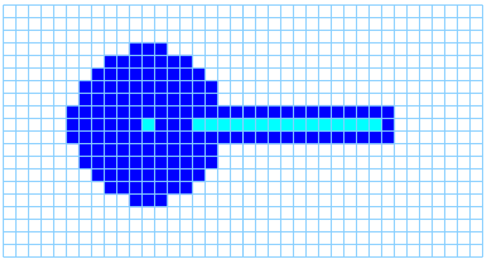

Figure 3: Non bounded disconnections with the Euclidean metric.

In order to avoid some of these problems, ([SGP96], [SGP93]) have proposed a continuous box-skeleton for discrete objects which preserves the homotopy, which does not have interior and whose shape is an abstract shape of the object. However, this skeleton does not converge to the Euclidean skeleton.

Next, an euclidian skeletal definition based on the Distance Map is proposed. It does not present discontinuities, it preserves the topological information and it is a complete representation scheme.

3 Discrete Medial Axis Transform

Before presenting the theory in the rest of section 3, the main underlying ideas are first outlined. This will hopefully help to better understand the motivation for the mathematics (see Figure 4).

Let O be a continuous object of $\Re^2$ and $MA_c(O)$ be its medial axis. According to [SPW96], if O is path-connected, then $MA_c(O)$ is also path-connected. Let $Discr(O)$ be the discretization of O in Z^2 and $Discr(MA_c(O))$ be the wrapping discretization of $MA_c(O)$. Finally, let $skeleton(Discr(O))$ be the skeleton of O as introduced in Definition 3 using the Euclidian metric. It would be expectable for $skeleton(Discr(O))$ to be equal to $Discr(MA_c(O))$, because both have been constructed using the same criterion, i.e., as the sets of centers of maximal disks. However, some maximal continuous disks may be rasterized into non-maximal discrete disks. Thus, $Discr(MA_c(O))$ and $skeleton(Discr(O))$ may not be equivalent, instead, $skeleton(Discr(O))$ is a subset of $Discr(MA_c(O))$. Furthermore, as stated in proposition 1, $skeleton(Discr(O))$ may not be connected.

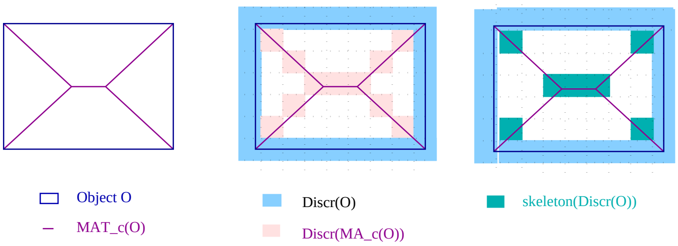

Figure 4: Underlying ideas about the $MA_d(Discr(O))$ definition.

The inequality between these two sets, $skeleton(Discr(O))$ and $Discr(MA_c(O))$, is caused by the two discretizations performed: the spatial one (R^2 on Z^2) and the metric one (the continuous radii on the discrete Euclidean metric).

As mentionned above, the goal of this report is to propose a connected discrete skeleton based on the Euclidian metric. This Discrete Medial Axis will therefore be defined as a connected subset of $Discr(MA_c(O))$ that encloses $skeleton(Discr(O))$ and thus guarantees both its completeness and its connectivity.

The problem addressed in the following sections is the characterization of the pixels of the connected Discrete Medial Axis. It will be proved that these pixels may be either centers of maximal disks or they fullfil specific properties of tangencies between disks that no other pixel of a discrete object fullfils. The definition of the $MA_d(Discr(O))$ as well as the proofs of its properties will therefore be derived from an analysis of the relationships between continuous and discrete objects and a study of the tangencies properties.

3.1 Reduction of the problem

Let $MA_c(O)$ be the Continuous Medial Axis of a continuous object O with boundary $bound(O)$:

$$\begin{aligned} MA_c(O) = \{ \quad & (x,y) \in \Re^2 / \quad (x,y) \in O \; \& \\ & \exists \epsilon > 0 : \quad dist((x,y), bound(O)) >= dist((x,y) \pm \epsilon, bound(O))\} \end{aligned}$$

The points of $MA_c(O)$ can be classified as CI (points with tangent continuity) and CII (points without tangent continuity) (see [Ver94]). Thus, $MA_c(O)$ is composed by the union of segments limited by CII points. All of these segments define a set of points which are centers of maximal disks inscribed into the object. These centers can be clustered in pairs such that their associated disks have a non-empty intersection area (see Figure 5).

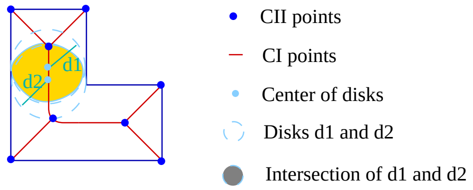

Figure 5: $MA_c(O)$ with CI and CII points.

It is possible to assume, without loss of generality, that the Continuous Medial Axis between every pair of inscribed maximal disks, $D_1(p_{x_1y_1})$ and $D_2(P_{x_2y_2})$ is equivalent to the Continuous Medial Axis of the object which is defined by the union of these pairs of disks $D_1(p_{x_1y_1}) \cup D_2(p_{x_2y_2})$.

For this reason, the general case of any discrete object may be reduced to the discretization of a continuous object O_u defined as the union of two intersecting disks, non enclosed one into each other, of centers (x_1, y_1) and (x_2, y_2) respectively and of radii r_a and r_b.

The following considerations must be taken into account:

- One continuous disk is discretized in the integer space using the Euclidean metric, as a set of one or more discrete disks. In section 3.2, the relationships between the disks of the two spaces are analyzed.
- The discretization of the metric produces that some tangencies between continuous disks change in the discrete metric. New discrete tangencies concepts are defined in section 3.3.
- The pixels of the discretization of the medial axis of the continuous object O_u fullfil some tangency properties between the disk and the boundary of the object. This case is analyzed in section 3.4.

3.2 Relationships between continuous disks and discrete disks

In this section, the discretization of the continuous space and of the continuous metric is analyzed in order to define the relationships between the continuous and the discrete disks.

The space R^2 of the continuous object O and its Continuous Medial Axis $MA_c(O)$ is discretized in Z^2. The center of a disk can be interior to a pixel, on an edge of the pixel or on one of its vertices (see Figure 6). The distance between the center of the disk and the center of the pixel is labelled as d and it is bounded by $0 \le d \le \frac{\sqrt{2}}{2}$.

The distance of each point of every pixel is collapsed to the distance of the center of the pixel. The error introduced in this process is $\epsilon_1 = d$.

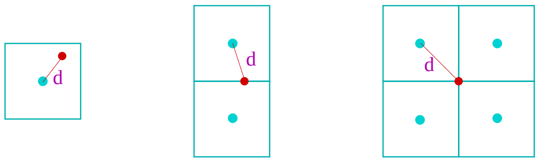

Figure 6: Locus of a point in relation to a pixel.

The distance values associated to the centers of the pixels are discretized by the Euclidian Distance ([Dan80]). This new labelling produces an error $\epsilon_2 = DM(r) - r$. The Euclidean Distance can be expressed as:

$$DM(r) = minimum_d\{d^2 = x^2 + y^2 / \ r \leq d \ \& \ x \in Z \ \& \ y \in Z\}$$

A continuous disk d_1 with center c and radius r is discretized in the integer space with the Euclidean metric as the union of at most 4 connected discrete maximal disks. This derives only from the analysis of the error ϵ_1, which measures the distance from the center of the continuous disk inside a pixel to the center of the pixel. If the center of the continuous disk falls on the exact center of the pixel, the discretization will consist of only one discrete disk whose center will be the pixel, even if the error ϵ_2 reaches its maximum value. If, on the contrary, ϵ_1 is larger than zero, it is at most $\sqrt{2}/2$, i.e. the center falls in a vertex of the pixel. Therefore, on the basis of the circle symmetry, in this case, the pixels inside the disk which are at maximum distance from the boundary will be at most 4.

The inverse relation, i. e. a discrete disk represents several continuous disks, is defined through the following properties. The Euclidean distance function $DM(r)$ can be expressed as the sequence S of integer numbers whose square is the sum of the square of two positive integers:

$$S \quad = \quad \{k \ / \ k = x^2 + y^2, \ x \in Z, \ y \in Z \ \} \tag{1}$$

Every element of S can be expressed as the product of its factors. An integer value k belongs to S if and only if all the factors larger than two and with odd exponent are congruent with 1 mod 4. This property can be expresed also as:

$$k = 2^a \times k' \ with \ k' \equiv \ 1(mod \ 4)$$

Then, it is possible to define the successor of any element r in S according to the value a of the exponent:

$$\begin{array}{lll} if \ a \geq 2 & then & succ(k) = k + 1 \\ if \ a = 1 & then & succ(k) = k + 2 \ or \ succ(k) = k + 3 \\ if \ a = 0 & then & succ(k) = k + 1 \ or \ succ(k) = k + 3 \ or \ succ(k) = k + 4 \end{array}$$

Property 1. *Let $DM(r)$ be the discretization of a continuous radius r, then $DM(r)$ defines an interval of possible continuous radii such that their discretization is $DM(r)$. These radii are bounded between $DM(r)$ and its predecessor in the sequence S (defined in the Equation 1).*

This property is ilustrated in the Figure 7.

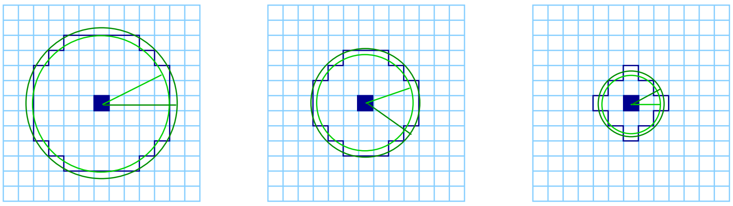

Figure 7: Radii interval defined by $DM(r)$.

3.3 Tangency properties

As the $DM(r)$ defines a discretization of a set of continuous disks whose discrete shape is the disk defined by $DM(r)$, it is possible to find continuous disks that intersect in R^2 but whose discretizations do not intersect in Z^2. Even more, their discretizations can be included one in the other.

3.3.1 Labelled subdisks

From the Euclidian distance associated to a pixel $p_{i'j'}$ of an Euclidean disk $D_t(p_{ij})$, the following subset of pixels is defined:

Def 4. Pixels Interior to a Disk, $PINT(D_t(p_{ij}))$, are all pixels $p_{i'j'}$ such that:

$$(i' - i)^2 + (j' - j)^2 \leq t^2$$

At least one pixel belonging to $\overline{PINT(D_t(p_{ij}))}$ exists whose distance is exactly t^2. There are at most 12 pixels which are exactly at distance t^2 (such as the disks: (5, 0), (3, 4) in Figure 8). The pixels located exactly at t^2 are called **pivot pixels**.

Let $D_t(p_{ij})$ be a disk centered at p_{ij} and with radi t, and let $p_{i'j'}$ a pixel inside $D_t(p_{ij})$, then the Distance Map associated to $p_{i'j'}$ defines a subdisk, $SD_{t'}(p_{i'j'}/D_t(p_{ij})$ inside $D_t(p_{ij})$ with center on $(i'j')$ such that $PINT(SD_{t'}(p_{i'j'})/D_t(p_{ij})) \in PINT(D_t(p_{ij}))$.

According to property 1, every subdisk $SD_{t'}(p_{i'j'}/D_t(p_{ij}))$ inside $D_t(p_{ij})$, being itself a disk, defines an interval of continuous radii. This interval intersects the interval of continuous radii defined by $D_t(p_{ij})$ (see Figure 9). The intersection arc is the union of the quadrant arc of the subdisk in relation with the disk and

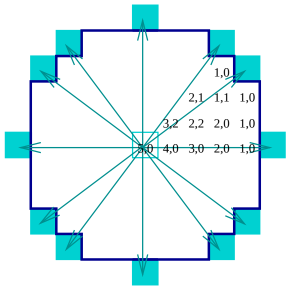

Figure 8: Example of pivot pixels in the case of the disk (5,0).

the arc bounded by the pivots of the subdisk. For any subdisk, the intersection arc defines the discrete tangency between the disk and the subdisk.

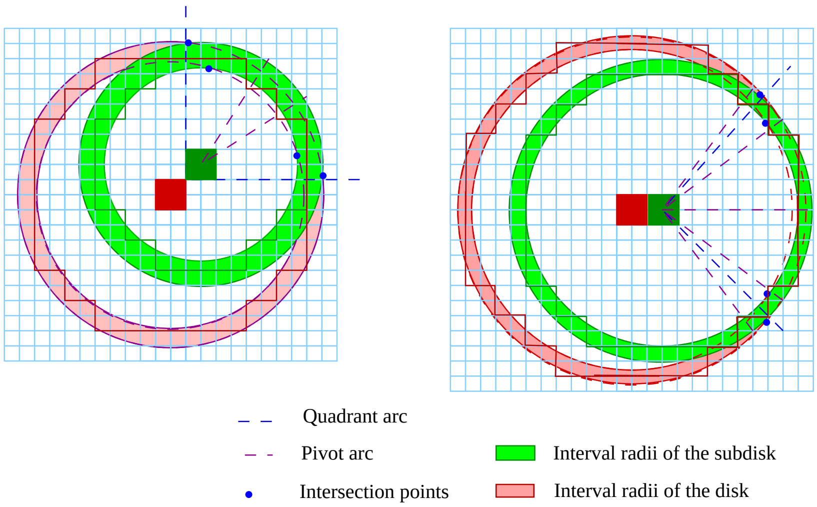

Figure 9: Arc of tangency between a disk and one of its subdisks.

Def 5. A Labeled Subdisk, $SD((p_{i'j'})/D_t(p_{ij}))$, is the subset of the pixels of $D_t(p_{ij})$ such that:

$$\begin{aligned} SD((p_{i'j'})/D_t(p_{ij})) \quad = \{p_{xy} \quad & / \ p_{xy} \in D_t(p_{ij}) \ \& \\ & p_{xy} \in \bigcup (quadrant((p_{i'j'})/(p_{ij})), pivot\_area(p_{i'j'})) \ \& \\ & LABEL(p_{x-i'\,y-j'}/D_{t'}(p_{i'j'})) = LABEL(p_{xy}/D_t(p_{ij}))\} \end{aligned}$$

where

$$
\begin{aligned}
LABEL(p_{xy}/D_t(p_{ij})) &= dist(p_{xy}, \overline{D_t(p_{ij})}) \\
quadrant_4(p_{ij}/p_{i_0j_0}) &= \{p_{i_1j_1} \\
& 0 \leq \frac{i_1 - i_0}{\sqrt{(i_1-i_0)^2+(j_1-j_0)^2}} \leq \frac{\sqrt{2}}{2} \\
& \&\ i_1 - i_0 \geq 0\} \\
quadrant_8(p_{ij}/p_{i_0j_0}) &= \{p_{i_1j_1} \\
& 0 \leq \frac{j_1 - j_0}{\sqrt{(i_1-i_0)^2+(j_1-j_0)^2}} \leq 1 \\
& \& j_1 - j_0 \geq 0\}
\end{aligned}
$$

being $p_{i_0j_0}$ the central pixel of the disk.

Only if the pixel is not a direct neighbour of the central pixel, the quadrant is defined as the intersection of all the quadrants corresponding to the pixels that have been labeled (see the Figure 10).

$$
quadrant(p_{ij}) = \bigcap_{c \in discs} quadrant_{4/8}(p_{ij}/p_{i_0j_0})
$$

$$
\begin{aligned}
pivot_{area}(p_{i'j'}) = \{ & p_{i_1j_1} \\
& (i_1, j_1) \in region(LABEL(p_{i'j'}/D_t(p_{ij}), (p_{i'j'})\}
\end{aligned}
$$

being $region(LABEL(p_{i'j'}/D_t(p_{ij})), (p_{i'j'}))$ the set of pixels which belong to the intersection area of the segments defined by the pivots of $LABEL(p_{i'j'}/D_t(p_{ij}))$ and the pixel $(p_{i'j'})$ (see Figure 11).

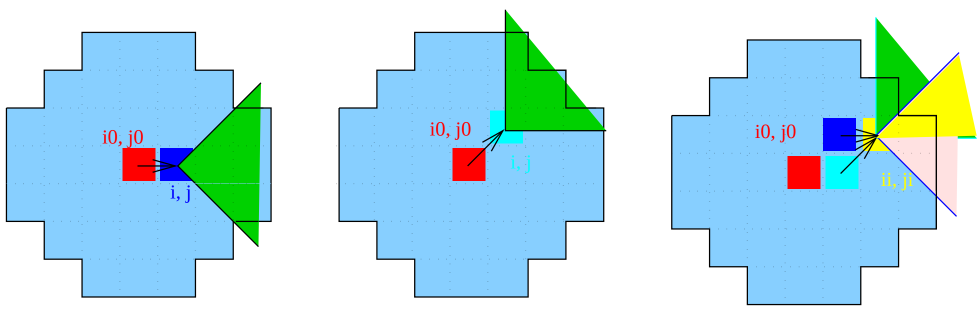

Figure 10: Representation of the quadrants of the subdisks.

This definition enables to specify the subarea of a disk in which subdisk is completely tangent to it.

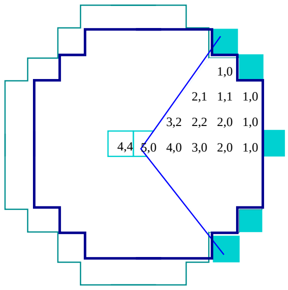

Figure 11: Representation of the $pivot(p_{i'j'})$ set.

3.3.2 PEX, REPR and TAP

The definitions that follow enable to determine the discrete tangency of two discrete objects. Specifically, they express the tangency of a maximal inscribed disk with the object and the tangency of a subdisk with its disk.

First, the dual set of $boundary(O)$ is defined.

Def 6. The **External Pixels of an object**, PEX, is the set of pixels which are not inside the object but which have a 8-neighbour that belongs to the object.

$$\begin{aligned} PEX(O) \quad &= \{p_{ij} / \quad \exists p_{i'j'} : p_{ij} \in 8neighbour(p_{ij}) \\ &\qquad such\ that\ \gamma(p_{i'j'}) = 1\ \&\ \gamma(p_{ij}) = 0\} \end{aligned}$$

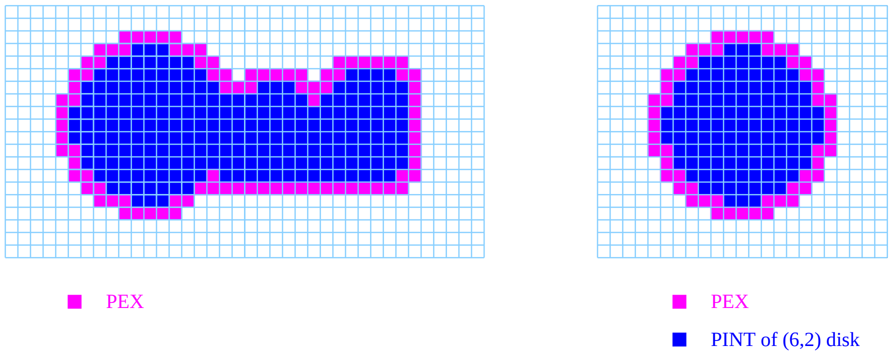

Figure 12: PEX and PINT sets.

According to this definition (see the Figure 12), for any discrete object $Discr(O)$, i.e. O_d, one PEX can be defined, also called $PEX(O_d)$, and for every disk $D_t(p_{ij})$ one PEX exists, $PEX(D_t(p_{ij}))$. Furthermore, in relation to the definition of PEX, it happens that:

1. Every maximal disk fitted inside the object O_d fullfils that:

$$PEX(O_d) \cap PEX(D_t(p_{ij})) \neq \phi$$

2. Let D_1 and D_2 be two disks, then they satisfy that $PEX(D_1) = PEX(D_2)$ only if $PINT(D_1) = PINT(D_2)$.

3. $PEX(D_1) \notin PINT(D_1)$.

4. If a pixel p_{ij} is interior to $D_t(p_{ij})$ and its associated distance map is $LABEL(p_{i'j'}/D_t(p_{ij}))$, then the disk defined at $p_{i'j'}$, $D_s(p_{i'j'})$ fullfils that:

   - According to the definition of Distance Map:

$$\forall(p_{i'j'}) :(p_{i'j'}) \in PINT(D_t(p_{ij})) : \\ PEX(D_s(p_{i'j'})) \cap PEX(D_t(p_{ij})) \neq \phi.$$

   - $PEX(D_s(p_{i'j'})) \in PEX(D_t(p_{ij})) \cup D_t(p_{ij})$
   - Moreover, the PEX associated to the labeled subdisk $SD(p_{i'j'}/D_t(p_{ij}))$, if $D_s(p_{i'j'})$ is the disk defined by the Distance Map of $p_{i'j'}$, may be computed as:

$$PEX(SD(p_{i'j'}/D_t(p_{ij}))) = PEX(D_s(p_{i'j'})) \cap PEX(D_t(p_{ij}))$$

Thus, the set of boundary pixels represented by a maximal disk may be defined as:

Def 7. Pixels Represented by a maximal disk, $REPR(D_t(p_{ij}), O_d)$, is the set of pixels such that:

$$REPR(D_t(p_{ij}), O_d) = PEX(O_d) \cap PEX(D_t(p_{ij}))$$

Def 8. Pixels Not Represented by a maximal disk, $TAP(D_t(p_{ij}), O_d)$ is the set of pixels such that:

$$TAP(D_t(p_{ij}), O_d) = PEX(D_t(p_{ij})) - REPR(D_t(p_{ij}), O_d)$$

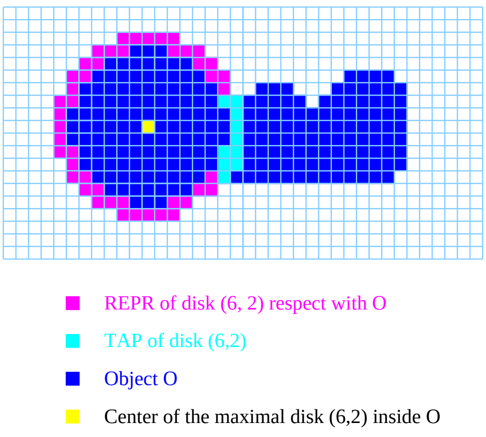

Figure 13: REPR and TAP sets.

These definitions and the properties are illustrated in the Figure 13. The main properties of the set $TAP(D_t(p_{ij}), O_d)$ are:

1. $TAP(D_t(p_{ij}), O_d) \notin PINT(D_t(p_{ij}))$.
2. Let O_d be a discrete object and let $D_t(p_{ij})$ be maximal disk interior to O_d, then:
   (a) If $TAP(D_t(p_{ij}), O_d) \neq \phi$ then $TAP(D_t(p_{ij}), O_d) \in PINT(O_d)$.
   (b) If $TAP(D_t(p_{ij}), O_d) = \phi$ then $PINT(D_t(p_{ij})) = PINT(O_d)$.
3. Given a disk $D_t(p_{ij})$, $\forall (i', j') : (p_{i'j'}) \in PINT(D_t(p_{ij}))$, then:
   (a) $TAP(SD(p_{i'j'}/D_t(p_{ij})), D_t(p_{ij})) \neq \phi$.
   (b) $TAP(SD(p_{i'j'}/D_t(p_{ij})), D_t(p_{ij})) \in PINT(D_t(p_{ij}))$.

From these definitions, the equivalent sets of a subdisk of any disk can be defined as $REPR(SD(p_{i'j'}/D_t(p_{ij})), O_d)$ and $TAP(SD(p_{i'j'}/D_t(p_{ij})), O_d)$.

3.4 Union of two continuous disks

Let O_u be a continuous object defined by the union of two intersecting disks D_1 and D_2 of centers (x_1, y_1) and (x_2, y_2) respectively and of radii r_a and r_b. The Continuous Medial Axis of O_u is the straight-line segment between the two centers and every maximal disk associated to every point of this segment fullfils one of the two following properties:

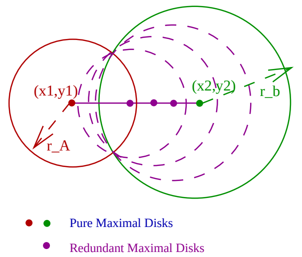

Figure 14: Continuous Medial Axis of two continuous disks.

- The maximal disk defines at least one point on the object's boundary that no other maximal disk defines. Then it is a Pure Maximal Disk.
- Or, all the points of the object boundary defined by the maximal disk have been defined by another maximal disk. Then it is a Redundant Maximal Disk, because it does not give any new information on the object.

It should be noted that all the continuous maximal disks of the object O_u intersect with other maximals but they are never tangent to another maximal disk (see Figure 14).

The analysis that follows has been done with straight-line segments whose slope is in the first octant, but it can be generalized to any other octant.

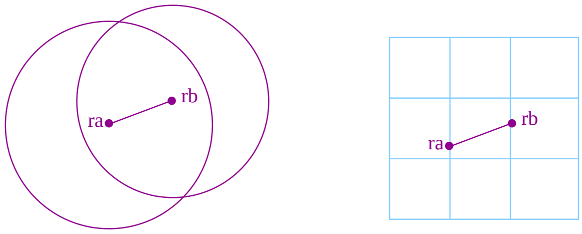

Figure 15: The O_u object and the pixel where the segment $(x_1, y_1) - (x_2, y_2)$ falls.

If the discretization of O_u is such that (x_1, y_1) and (x_2, y_2) fall into the same pixel (see Figure 15) and the Continuous Medial Axis of O is a straight-line segment, then there is a finite set of possible discretizations of the continuous axis, depending on the rasterizations of the r_a and r_b.

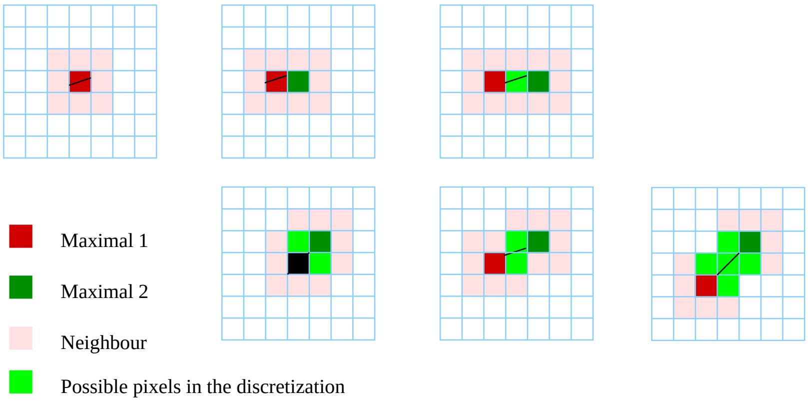

Figure 16: One maximal.

There are several cases depending on the number of maximals and non maximals that r_a and r_b can produced on the discretization. The set of these finite cases has been analyzed and it is depicted in Figures 16, 17, 18, 19. The two first figures show the cases in which r_a and r_b both generate maximal disks.The pixels of the discretization on the neighbour of these maximals are explored and classified according their tangency properties. In the simpler case, the interval of radii defined between r_a and r_b is discretized into only one maximal disk.

The two last figures illustrate cases in which only one non maximal or two non maximal are generated from a maximal. The neighbourhood analyzed is composed by the pixels of the discretization 8-connected to the non-maximals. A non-maximal pixel is the center of a disk which is necessarily enclosed into at least one maximal disk. The center of any disk to which a non-maximal pixel belongs will be called *owner* of the pixel.

The connected set of pixel defined by the discretization can be subdivided into waves. Let m to be the slope of a continuous straight line and let $\bar{dir}$ be the most influent direction of the slope m, a $wave(p_{ij}, \bar{dir})$ of this continuous straight line in a pixel p_{ij} of its discretization is the connected set composed

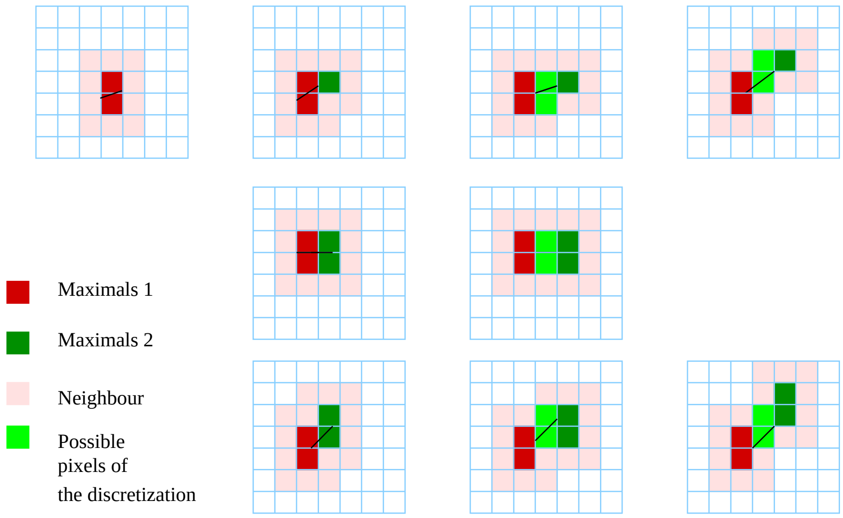

Figure 17: Two maximal.

by the intersection of the discretization of the straight line segment and the coordinate direction $\bar{dir}$ that passes through the pixel next to p_{ij} in direction $\bar{dir}$ (see Figure 20).

Synthetising, a wave of the discretization of a continuous axis is composed by:

1. Only one pixel which is the center of a discrete maximal disk (M1).
2. Two pixels that are the centers of two discrete maximal disks (M2).
3. Only one pixel which is center of a discrete non-maximal disk and which has the same TAP than all its owners on any wave of the discretization (NM1).
4. Two pixels that are centers of two discrete non-maximal disks such that the union of their associated TAP recovers the TAP of their owner (NM2). The associated TAP to the two non-maximals disks is defined according to the following assumption. The PEX of the object formed by the union of two disks which have connected centers is the set of pixels that are out of the union and that have an 8-connected neighbour inside the union. The TAP of this union is defined from this PEX, not as the TAP of the two corresponding PEX sets.
5. A pixel which is center of a discrete maximal disk with a non-maximal disk that does not cover the TAP of its owner (M1+NM3).

Extrapolating the conclusions from the former situation, if the discretization of O_u is such that (x_1, y_1) and (x_2, y_2) do not fall into same pixel, the discretization of the continuous straight line axis is obviously a connected set of pixels.

Conversely, no other pixel outside the waves of the discretization of a continuous axis can be center of a maximal disk, and they cannot either cover, by themselves or with one neighbour, the TAP of their owner.

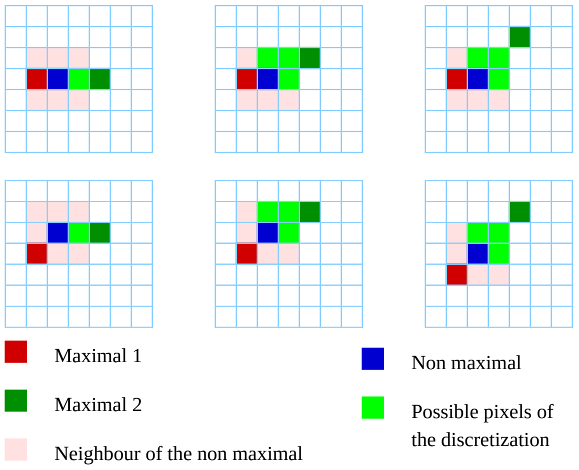

Figure 18: One non-maximal.

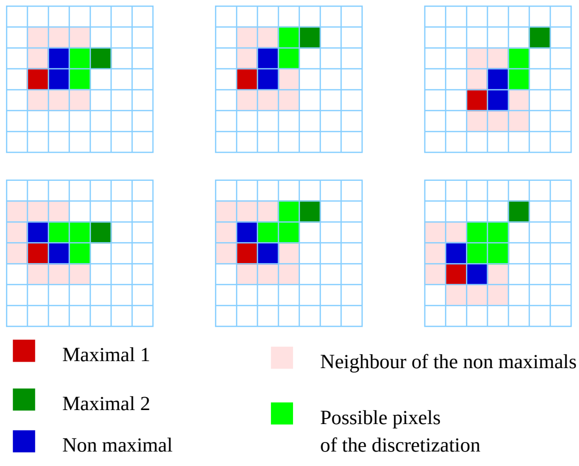

Figure 19: Two non-maximal.

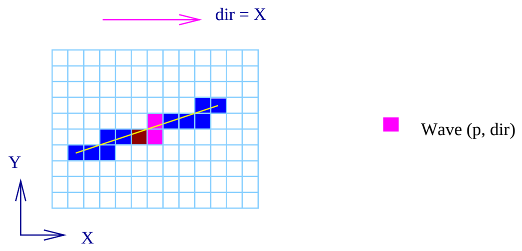

Figure 20: Illustration of a wave.

3.5 Discrete Medial Axis

Def 9. The **Discrete Medial Axis** $MA_d(O_d)$ of a discrete object O_d, is the set of the pixels belonging to the closure of the centers of the maximal disks incribed into the domain of the discretization plus the set of pixels which are centers of non-maximal disks sharing their non-represented pixel set with the maximal disk to which they belong.

$$\boxed{MA_d(O_d) = \{p_{ij}/(p_{ij}) \in closure(center(maximal\_disk) \cup sharing\_points)\}}$$

where,

$$\begin{aligned}
maximal_disk &= \{disk/\ \nexists d:\ disk \in d\} \\
sharing_points &= \{(p_{ij})/(p_{ij}) \in maximal_disk(p_{xy})\ such\ that \\
&\quad TAP(SD(p_{ij})/D_t(p_{xy}), O_d) = TAP(D_t(p_{xy}), O_d)\ \| \\
&\quad \exists (i'j') : p_{i'j'} \in maximal_disk(p_{xy})\ such\ that \\
&\quad TAP(SD(p_{ij}) \cup SD(p_{i'j'})/D_t(p_{xy}), O_d) = TAP(D_t(p_{xy}), O_d)\ \| \\
&\quad \exists (x'y') : TAP(SD(p_{ij}) \cup SD(p_{i'j'})/(D_t(p_{xy}) \cup D_{t'}(p_{x'y'}), O_d) = \\
&\quad TAP(D_t(p_{xy}) \cup D_{t'}(p_{x'y'}), O_d)\}
\end{aligned}$$

The intuitive idea underlying the principle of sharing pixels is that they connect successive maximal disk center pixels.

Then, the **Discrete Medial Axis Transform** of an object $DMAT(O_d)$ is a pair $< MA_d(O_d),\ dist(MA_d(O_d)) >$, where $MA_d(O_d)$ is the Discrete Medial Axis of the object and $dist(MA_d(O_d))$ is a function which assigns the Euclidean distance at each pixel belonging to $MA_d(O_d)$.

3.6 Properties of the Discrete Medial Axis

The main properties of the Discrete Medial Axis are:

Proposition 2. *The Discrete Medial Axis of a discrete 4-path-connected object is 8-connected.*

Proof. The Continuous Medial Axis of a path-connected object is path-connected ([SPW96]).

The discretization of a path-connected object is a discrete path-connected object. The wrapping discretization of the continuous Medial Axis is a 4-connected set of pixels.

The Discrete Medial Axis is a subset of the Continuous Medial Axis of the object whose pixels which do not belong to the $MA_d(O_d)$ are well-characterized (NM3 pixels of M1+NM3 case in the section 3.4). These pixels always belong to a wave of the 4-connected discretization that is formed almost by one maximal. Then, the $MA_d(O_d)$ is a 8-connected set only is O_d is 4-path-connected. □

Proposition 3. *The Discrete Medial Axis of a discretization of a continuous object is a subset of the discretization of an Continuous Medial Axis of the continuous object O.*

$$\boxed{MA_d(Discr(O)) \subseteq Discr(MA_c(O))}$$

Proof. The $MA_d(Discr(O))$ is a subset of the discretization of the $MA_c(O)$ because there exist pixels on the discretization of the $MA_c(O)$ which not are in $MA_d(Discr(O))$. These pixels are non-maximal pixels which compose a wave of the $MA_c(O)$ together with one. These non-maximals do not fullfil any of the conditions of the DMA, i. e. they do not share their TAP with their owner. □

Property 2. *The width of the Discrete Medial Axis is at most of 2 pixels on the CII limited segments of the axis.*

Proof. It is trivial by the first property of the Discrete Medial Axis. □

Property 3. *The Discrete Medial Axis Transform is a complete representation scheme.*

Proof. Every point of the boundary is represented by some point of the Discrete Medial Axis Transform and it is also possible to reconstruct the boundary only from the information stored in the Discrete Medial Axis Transform. Specifically, [Dan80] has demonstrated the completeness of the subset of the maximals centers included in the definition 9. □

4 Building Algorithm

In this section, a building algorithm is proposed based on the properties of the Discrete Medial Axis Transform analyzed above. The core of the algorithm is a seed strategy. It starts with an initial pixel that is specified beforehand and which belongs to the Discrete Medial Axis of the analyzed object.

[Dan80] codifies all the pixels from a disk $D_t(p_{ij})$ according to their respective Distance Map, that is to say, every pixel of a disk $p_{i'j'}$ is labeled with the minimum value of the Euclidian distance to the boundary of the disk, $LABEL(p_{i'j'}/D_t(p_{ij}))$. Thus, it is feasible to build a lookup table to compact the disk information. Furthermore, the PEX set of every disk may be calculated in a lookup table in order to accelerate the algorithm.

At each stage, the seed function is divided into two main processes. First, the Distance Map at the current pixel is calculated and then, from this value, the ownership of the pixel to the Discrete Medial Axis is tested. The following seed function performs both processes:

Def 10. Let (p_{ij}) be a pixel of the Discrete Medial Axis of O_d and $D_t(p_{ij})$ its associated disk, then $f(p_{ij})$ is defined as:

$$
\begin{aligned}
f(p_{ij}) = \{ & p_{i_kj_k} / p_{i_kj_k} \in 8neighbour(p_{ij}) \ \& \\
& \nexists p_{i_sj_s} : \ p_{i_sj_s} \in 8neighbour(p_{ij}) : p_{i_kj_k} \in D_s(p_{i_sj_s}) \ \| \\
& sharing\_points(p_{i_kj_k}/p_{ij}) \}
\end{aligned}
$$

where

$$
\begin{aligned}
sharing\_points(p_{i_kj_k}/p_{ij}) \ = \ & \\
& \{ p_{i_kj_k} \in D_t(p_{ij}) \ \& \ TAP(p_{ij}, O_d) = TAP(p_{i_kj_k}, O_d) \qquad \| \\
& \exists p_{i_sj_s} : p_{i_sj_s} \in D_t(p_{ij}) : \\
& TAP(D_s(p_{i_sj_s}) \cup D_k(p_{i_kj_k}), O_d) = TAP(p_{ij}, O_d) \qquad \| \\
& \exists p_{i'j'} : \\
& TAP(SD(p_{i_sj_s}) \cup SD(p_{i_kj_k}) / (D_t(p_{ij}) \cup D_{t'}(p_{i'j'}), O_d) = \\
& TAP(D_t(p_{ij}) \cup D_{t'}(p_{i'j'}), O_d) \}
\end{aligned}
$$

Theorem 1. *The Discrete Medial Axis Transform of a 2D discrete object may be computed with the seed function defined in Definition 10.*

Proof. The proof is reduced to demonstrate that:

1. The function defined in 10 computes pixels that belong to the Discrete Medial Axis and only this type of pixels. This property is implicit in the Discrete Medial Axis definition.

2. The seed function is a local computation, i. e., the functions *sharing_points* and $D_t(p_{ij})$ may be calculated from local information of the neighbourhood of p_{ij}.

   The function *sharing_points* is computable using directly its definition in a local neighbourhood.

   To compute $D_t(p_{ij})$ is equivalent to calculate the associated Distance Map at p_{ij}. There are two ways to compute the Distance Map at a pixel. First, it can be calculated on a preprocess that realizes a doble scan of the image ([Dan80]). With this preprocess, which has a linear cost with the size of the image and it needs an additional image buffer, in the seed algorithm the computation is local. On the other hand, it is possible to calculate locally the Distance Map on the seed algorithm if the coherence of the Distance Map of a neighbour is used.

   Proposition 4. *Given a pixel p_{ij} and its associated Distance Map, the Distance Map of any neighbour of (p_{ij}) may be computed locally.*

   This proposition is demonstrated from the following two propositions, which can be validated directly:

   Proposition 5. *Given the Distance Map associated to a pixel, $DM(p_{xy}) = (i, j)$ such that $r = square(i^2 + j^2)$ is its module, then the Distance Map associated to some of its eight neighbour fullfils that:*

   $$2 \times min(i, j) - 1 \ < \ r \ \leq \ DM(r) \ < \ 2 \times min(i, j) + 1$$

Proposition 6. *The number of discrete disks of the interval where r' can vary is bounded by a function of r' and the upper bound of its square is 4.*

□

5 Cost

According to the explanations above, there are two strategies for the construction of the Discrete Medial Axis Transform: computing the Distance Map in a preprocess or computing it locally during the construction. In proposition 7 the former strategy cost is evaluated and the latter is analyzed in proposition 8.

Proposition 7. *The cost of the construction algorithm of the Discrete Medial Axis is $O_1(8 \times n + \#PINT(O_d) \times K_1)$, where n is the number of pixels of the initial image and $\#PINT(O_d)$ is the number of pixels which define the object. K_1 is the number of basic operations, such as additions or comparisons, and it is greater than 1.*

The first term of the sum is the cost of the Distance Map computation with a preprocess such as Danielsson's. The second term is the cost of the seed function. Therefore, the cost is linear with the number of pixels of the image. In the algorithm implemented, the value of K_1 is about 132 basic operations.

Proposition 8. *If the computation of the Distance Map is performed locally in each iteration of the seed algorithm, its cost is $O_2(\#PINT(O_d) \times (\pi \times d \times 2 + K_2))$, where d is the maximum diameter of the greater disk used.*

The cost of an algorithm to compute skeletals approximations such as Danielsson' s one is $O(8 \times n + 3 \times n \times (\#PINT(O_d) + 23 \times n))$. In general, the algorithm has a higher cost than a classical skeleton approximation. This is the price of guaranteing the connectivity of the skeleton. However, as all the costs are linear, in images where the ratio between the number of pixels of the image and the number of pixels of the object is low, such as thinned objects, the seed algorithm improves the scan algorithm. Therefore, the algorithm is especially suitable to extract connected skeletons of elongated structures.

6 Results on empirical data

The construction algorithm has been proved with sets of sinthetic images of different sizes and with different objects.

Run times for these analysis, using the same 512×512 pixels model trials, were about 33.2 seconds on average with a SunSparc 10 machine on the SunOS version 4.1.3 using 16 Mb RAM, 1Mb Cache at 40 MHz. The vascular tree image and its associated model are shown in Figures 21 and 22. Colour plate 23 is a zooming image of the previous case in which the skeleton is superposed onto the Distance Map.

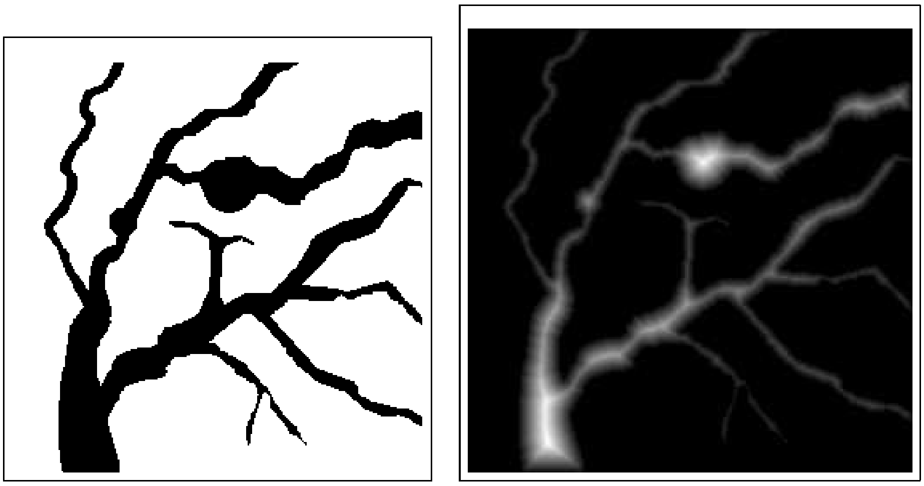

Figure 21: Input object and its Distance Map.

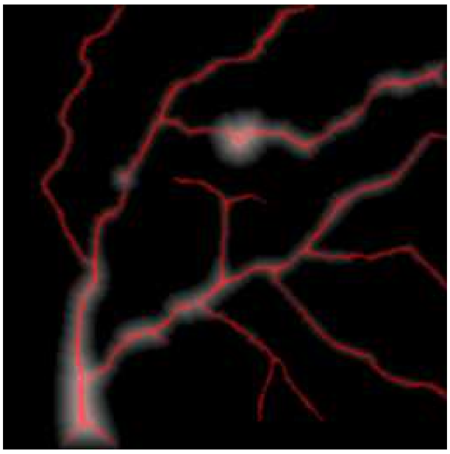

Figure 22: Example of extraction of Discrete Medial Axis

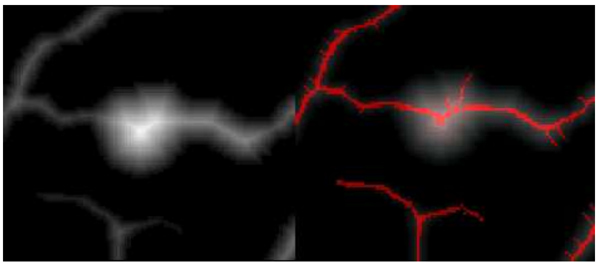

Figure 23: Zooming detail

7 3D Extension

As in the 2D case, several methods which extract skeletal approximations of 3D objects exist. They are, generally, extensions to 3D of thinning approaches [LKC94], [TF81]. However, they either do not preserve topology or the geometrical structure of the object. [GKS+93] generalizes Danielsson algorithm to 3D and obtains a disconnected medial axis approximation, without increasing the maximal distance error.

The 2D definition of the Discrete Medial Axis proposed in section 3 is extended to 3D on the basis of the 3D Medial Axis defined by [Blu67].

Let S be the surface of the boundary of an object, O, the **Continuous Medial Axis of** S is $MA_c(O)$ such that:

$$\begin{aligned} MA_c(O) = \quad & \{(x,y,z) \in \Re^3 / \quad (x,y,z) \in O \ \& \\ & \exists \epsilon > 0 : \quad dist((x,y,z),S) >= dist((x,y,z) \pm \epsilon, S)\} \end{aligned}$$

where $dist((x,y,z),S)$ is the minimum continuous Euclidean distance of the point (x,y,z) to the surface S.

Def 11. The **Discrete Medial Axis** $MA_d(O_d)$ of a discrete object O_d, is the set of voxels belonging to the closure of the centers of the maximal spheres incribed into the domain of the discretization plus the set of voxels which are centers of non-maximal spheres sharing their non-represented voxel set with the maximal sphere to which they belong.

$$\begin{aligned} MA_d(O_d) \ = \{ \ & v_{ijk}/ \\ & v_{ijk} \in closure(center(maximal\_sphere) \ \cup \ sharing\_points)\} \end{aligned}$$

where

$$\begin{aligned} maximal\_sphere \ = \quad & \{sphere/ \ \nexists e : \ sphere \in e\} \\ sharing\_points \ = \quad & \\ & \{v_{ijk}/v_{ijk} \in S_{3D_l}(v_{tsr}) \ maximal \\ & \ such \ that \\ & TAP_{3D}(SS_{3D}(v_{ijk}/S_{3D_l}(v_{tsr}), O_d)) = TAP_{3D}(S_{3D_l}(v_{tsr}), O_d) \ || \\ & \exists (i',j',k') : v_{i'j'k'} \in S_{3D_l}(v_{tsr}) \ such \ that \\ & TAP_{3D}(SS_{3D}(v_{ijk}) \cup SS_{3D}(v_{i'j'k'})/S_{3D_l}(v_{tsr}), O_d) = \\ & TAP_{3D}(S_{3D_l}(p_{tsr}), O_d) || \\ & \exists v_{t's'r'} : \\ & TAP_{3D}(SS_{3D}(v_{ijk}) \cup SS_{3D}(v_{i'j'k'})/S_{3D_l}(v_{tsr}) \cup S_{3D'_l}(v_{t's'r'}), O_d) = \\ & TAP_{3D}(S_{3D_l}(v_{tsr}) \cup S_{3D'_l}(v_{t's'r'}), O_d)\} \end{aligned}$$

where the spheres $S_{3D_l}(p_{ijk})$, the sets TAP_{3D} and the subspheres SS_{3D} are the natural extension to 3D of the concepts of disks, TAP and subdisks. The underlying idea of the sharing voxels is the connectness between centers of maximal spheres.

Obviously, the metric used is the Euclidean distance defined by [Dan80] extrapolated to 3D. It is possible to label each voxel interior to a sphere with its associated Distance Map as $LABEL(p_{i'j'k'}/S_{3D_l}(p_{ijk}))$.

The property of the equivalence of the Discrete Medial Axis of a discretization of an object and the discretization of the Medial Axis of the object is valid as in the 2D case. Therefore, the 28-path-connectivity of the Discrete Medial Axis, its completeness and its minimum witdh are also valid characteristics of the 3D Discrete Medial Axis.

The algorithm presented in section 4 is extended to 3D. The complexity of the construction algorithm still remains $O_1(K_1 \times n + K_2 \times \#PINT(O_d))$ and the cost of the computation of the Distance Map at each voxel is $O_2(\#PINT(O_d) \times (\pi \times d^2/2 + K_3))$, where n is the number of voxels of the initial 3D image, $\#PINT(O_d)$ is the number of voxels inside the object and d is the maximum diameter of the greater sphere used.

8 Conclusions and future trends

A new definition of a Discrete Medial Axis which provides 8-connectivity, low thickness and model completness is proposed. As it is a Medial Axis, it provides dimensionality reduction, symmetry detection and invertibility. It preserves the topological characteristics of the object. The Medial Axis is sensitive to border noises, therefore, in some applications it is necessary to detect this noise in order to find some relevant characteristics of the analyzed object.

An efficient seed algorithm that requires a number of passes proportional to the dimensions of the object has been described. This algorithm is better on thinned objects or on objects whose radius respect with the size of the image is low. It is well suited for applications such as data compression, image analysis, character recognition and circuit inspection.

By a simple extension, the definition and the algorithm can be applied to the 3D space. It can be useful in applications such as pattern recognition of thinned structures on large images. Another application is the extraction of a model of elongated anatomical structures such as blood vessels, intestines or the colon in medical images. Similarly, it may be used for the detection of rivers and roads in Geographical Information Systems.

Within these different applications, work is currently underway to apply this method to real 3D angiograms images. A current research line is the improvement of the algorithm using coherent information between two consecutives steps of the seed. The additional data provided by the bisectrice defined by a maximal disk may also be used in order to cull-off pixels in the navigation of the building algorithm.

References

[Blu67] H. Blum. A transformation for extracting new descriptors of shape. *Models for the Perception of Speech and Visual Form. MIT Press, Cambridge, Mass.*, pages 362–380, 1967.

[Bor84] G. Borgefors. Distance transformations in arbitrary dimensions. *Computer Vision, Graphics and Image Processing*, 27:321–345, 1984.

[Bor86] G. Borgefors. Distance transformations in digital images. *Computer Vision, Graphics and Image Processing*, 34:344–371, 1986.

[CCS95] S.S.O. Choy, C.S.T. Choy, and W.C. Siu. New single-pass algorithm for parallel thinning. *Computer Vision and Image Understanding*, 62(1):69–77, July 1995.

[Chi92] C.S. Chiang. *The Euclidean Distance Transform.* PhD thesis, Purdue University, Department of Computer Science, August 1992.

[Dan80] P.E. Danielsson. Euclidean distance mapping. *Computer Graphics and Image Processing*, 14:227–248, 1980.

[GKS+93] G. Gerig, Th. Koller, G. Szkely, Ch. Brechbhler, and O. Kbler. Symbolic description of 3-d structures applied to cerebral vessel tree obtained from mr angiography volume data. *Proceedings of the 13th International Conference on Information Processing in Medical Imaging, Springer-Verlag, New York/Berlin*, pages 94–111, 1993.

[KR89] T.Y. Kong and A. Rosenfeld. Survey: Digital topology: Introduction and survey. *Computer Vision, Graphics and Image Processing*, 48:357–393, December 1989.

[KSKB95] R. Kimel, D. Shaked, N. Kiryati, and A.M. Bruckstein. Skeletonization via distance map and level sets. *Computer Vision and Image Understanding*, 62(3):382–395, November 1995.

[LKC94] T.C. Lee, R.L. Kashyap, and C.N. Chu. Building skeleton models via 3-d medial surface/axis thinning algorithms. *CVGIP: Graphical Models and Image Processing*, 56(6):462–478, November 1994.

[LLS92] L. Lam, S.W. Lee, and C.Y. Suen. Thinning methodologies - a comprehensive survey. *IEEE Transactions on Pattern Analysis and Machine Intelligence*, 14(9):869–885, September 1992.

[MMD96] Y. Masutani, K. Masamune, and T. Dohi. Region-growing based feature extraction algorithm for tree-like objects. *Proceedings of 4th International Conference Visualization in Biomedical Computing, Hamburg, Germany*, pages 161–171, September 1996.

[ND97] F. Nilsson and P.E. Danielsson. Finding the minimal set of maximum disks for binary objects. *Graphical Models and Image Processing*, 59(1):55–60, January 1997.

[SGP93] A. Sudhalkar, L. Grsz, and F. Prinz. Continuous skeletons of discrete objects. *ACM Proceedings on Solid Modelling 93, Montreal, Canada*, pages 85–94, 1993.

[SGP96] A. Sudhalkar, L. Grsz, and F. Prinz. Box-skeletons of discrete solids. *Computer-Aided Design*, 28(6/7):507–517, 1996.

[SPW96] E.C. Sherbrooke, N.M. Patrikalakis, and F.E. Wolter. Differential and topological properties of medial axis transforms. *Graphical Models and Image Processing*, 58(6):574–592, November 1996.

[TF81] Y.F. Tsao and K.S. Fu. A parallel thinning algorithm for 3-d pictures. *Computer Graphics and Image Processing*, 17:315–331, 1981.

[Ver94] P.J. Vermeer. Medial axis transform to boundary representation conversion. *PhD Thesis, Purdue University*, May 1994.